Mu-21: A Three-Dimensional Microporous Zincophosphate Obtained by Direct Synthesis and Reversible Dehydration of the Zincophosphate Mu-19

Angélique Simon-Masseron,* Jean-Louis Paillaud, and Joël Patarin

Laboratoire de Matériaux Minéraux, UMR CNRS 7016, Ecole Nationale Supérieure de Chimie, Université de Haute-Alsace, 3 rue Alfred Werner, 68093 Mulhouse Cedex, France

Received October 8, 2002. Revised Manuscript Received December 2, 2002

A zincophosphate named Mu-21 ($Zn_4P_8O_{32}H_{12}(C_5H_{12}NO)_4$) was obtained in solvothermal conditions from a ZnO/H_3PO_4/*N*-methylmorpholine/ethylene glycol mixture, and its structure was solved ab initio from powder data. Mu-21 crystallized in the orthorhombic space group P $2_12_12_1$ with $a = 10.4200(1)$, $b = 10.4523(2)$, $c = 11.6221(2)$ Å, and $V = 1265.80(3)$ Å^3. Mu-21 was also obtained by reversible dehydration of the zincophosphate Mu-19 at 80 °C. This material was characterized by ^{31}P, ^1H MAS NMR, and SEM.

1. Introduction

Since the first syntheses of microporous zincophosphates in 1991 by Gier and Stucky[1] and Harrison et al.,[2] more than 120 new zincophosphate structures have been discovered.[3] The interest for this type of microporous phosphates has increased considerably in the past five years (Figure 1). Such an evolution may be explained by the rich diversity of structures that can be found in this system and the low temperature conditions of synthesis. These materials display one-, two-, or three-dimensional structures which are built mainly from ZnO_4 and PO_4 tetrahedral, and more rarely by ZnO_6 and ZnO_5, subunits.[4] Some zincophosphates are structurally related to zeolite-type materials[5] and present catalytic properties like those of the zincophosphates with the FAU (faujasite) and CZP (chiral zincophosphate) structure-types which present an interesting activity in the base-catalyzed Knoevenagel condensation of benzaldehyde and methylenic compounds.[6] However, most zincophosphates have a low thermal stability and their structure changes after water adsorption.

In the present paper, the synthesis and the characterization of a new zincophosphate named Mu-21 is described. This material can be obtained by direct synthesis in an aqueous or a quasi-nonaqueous medium (ethylene glycol as solvent), and also by dehydration of the previously obtained zincophosphate Mu-19.[7]

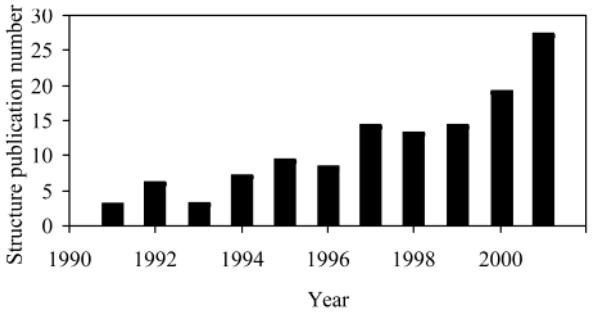

Figure 1. Evolution of the number of publications devoted to new microporous zincophosphate structures (1-D, 2-D, and 3-D) per year.

2. Experimental Section

2.1 Synthesis. As an example for sample A (Table 1), Mu-21 was prepared from a mixture composed of 1.02 g of ZnO (Carlo Erba, 99%), 5.68 g of H_3PO_4 (Labosi, 85%), and 3.27 g of *N*-methylmorpholine (Aldrich, 99%) introduced in 12.33 g of ethylene glycol (EG, SDS, synthesis grade). The starting mixture with the molar ratio 0.5 ZnO:1 P_2O_5:7.9 EG:1.3 template:1.9 H_2O was kept at room temperature for 17 days. The recovered white crystalline product was rinsed with 10 mL of ethanol and dried overnight at 60 °C. The washing procedure appears to be critical because this zincophosphate transforms into the zincophosphate tetrahydrate hopeite $Zn_3(PO_4)_2{\cdot}4H_2O$ on washing with water.

2.2 Characterization. The powder XRD pattern was obtained using the Cu $K\alpha_1$ radiation on a STOE-STADI-P diffractometer equipped with a curved germanium (111) primary monochromator and a linear

* To whom correspondence should be addressed via e-mail: A.Simon@univ-mulhouse.fr.

(1) Gier, T. E.; Stucky, G. D. *Nature* **1991**, *349*, 508−510.

(2) Nenoff, T. M.; Harrison, W. T. A.; Gier, T. E.; Stucky, G. D. *J. Am. Chem. Soc.* **1991**, *113*, 378−379.

(3) For example: (a) Nenoff, T. M.; Harrison, W. T. A.; Gier, T. E.; Calabrese, J. C.; Stucky, G. D. *J. Solid State Chem.* **1993**, *107*, 285−295. (b) Wallau, M.; Patarin, J.; Widmer, I.; Caullet, P.; Guth, J. L.; Huve, L. *Zeolites* **1994**, *14*, 402−410. (c) Marler, B.; Patarin, J.; Sierra, L. *Microporous Mater.* **1995**, *5*, 151−159. (d) Reinert, P.; Zabukovec Logar, N.; Patarin, J.; Kaucic, V. *Eur. J. Solid State Inorg. Chem.* **1998**, *35*, 373−387. (e) Neeraj, S.; Natarajan, S.; Rao, C. N. R. *J. Chem. Soc., Dalton Trans.* **2001**, 289−291.

(4) Harrison, W. T. A.; Vaughey, J. T.; Dussack, L. L.; Jacobson, A. J.; Martin, T. E.; Stucky, G. D. *J. Solid State Chem.* **1995**, *114*, 151−158.

(5) (a) Harrison, W. T. A. *Int. J. Inorganic Mater.* **2001**, *3*, 179−182. (b) Neeraj, S.; Natarajan, S. *J. Phys. Chem. Solids* **2001**, *62*, 1499−1505. (c) Harrison, W. T. A. *Acta Crystallogr., Section E, Structure Reports Online* **2001**, *57*, 248−250.

(6) Garcia-Serrano, L. A.; Blasco, T.; Pérez-Pariente, J.; Sastre, E. *13th International Zeolite Conference*; Montpellier, France, 2001.

(7) Simon, A.; Josien, L.; Gramlich, V.; Patarin, J. *Micropor. Mesopor. Mater.* **2001**, *47*, 135−146.

10.1021/cm021330g CCC: $25.00
Published on Web 01/28/2003

Table 1. Synthesis Conditions for the Zincophosphate Mu-21

	gel composition (molar ratio)							
sample	ZnO	P_2O_5	H_2O	$CH_3(C_4H_8NO)$	HF	$HOCH_2CH_2OH$	*T* (°C)	time (d)
A	0.5	1	6.8	1.2			RT[a]	20
B	0.5	1	1.9	1.3		7.9	RT	17
C	0.5	1	6.8	1.2	0.2		RT	19

[a] Room temperature.

Table 2. Summary of the Experimental and Crystallographic Data of the Zincophosphate Mu-21

unit cell formula	$Zn_4P_8O_{32}H_{12}(C_5H_{12}NO)_4$
calculated unit cell formula weight (g)	1441.963
space group	P 2_1 2_1 2_1
a (Å)	10.4200(1)
b (Å)	10.4523(2)
c (Å)	11.6221(2)
volume (Å^3)	1265.80(3)
density (calculated) (g ml^{-3})	1.892
number of contributing reflections	387
number of structural parameters	109
number of profile parameters	13
[a] $R_p = \sum\{[\lvert y_o - y_c\rvert \times \lvert y_o - y_b\rvert/y_o]/\sum\lvert y_o - y_b\rvert\}$	0.0370
[a] $wR_p = \{\sum[w \times (y_o - y_c) \times (y_o - y_b)/y_o]^2/\sum[w \times (y_o - y_b)^2]\}^{1/2}$	0.0459
[b] R_{exp}	0.0206
[b] R_F	0.0326
[b] R_F^2	0.0569
[b] χ^2	6.362
largest diff. peak and hole (e·Å^{-3})	0.322, −0.256

[a] y_o, y_c, y_b are y observed, y calculated, and y background, respectively. [b] The definitions of these residual values are given in ref 10.

Table 3. Recording Conditions of the MAS NMR Spectra

	^1H	^{31}P
chemical shift standard	TMS	85% H_3PO_4
frequency (MHz)	400.14	161.98
pulse width (μs)	5.5	4.5
flip angle	$\pi/2$	$\pi/2$
spinning rate (Hz)	8	8
number of scans	16	12 or 300
recycle time (s)	10	1032 or 6

position sensitive detector. The powder was introduced in a 0.3-mm glass capillary. The unit cell parameters were determined using the Werner's trial-and-error indexing program.[8] For the structure determination the extracted intensities of the reflections up to 60° 2θ (d = 1.540 Å) were taken; whereas for the Rietveld refinement the complete pattern (5−72°) was used. The structure of Mu-21 was solved using the EXPO[9] software (an ensemble of structure determination programs) and hereafter, the Rietveld refinement was performed using the GSAS[10] package. The experimental and crystallographic data are summarized in Table 2.

The ^{31}P T_1 relaxation times were measured using the inversion−recovery pulse sequence with incremented delay varying from 50 to 600 ms and 256 scans for each spectrum. The other recording conditions of the ^{31}P and ^1H MAS NMR spectra are given in Table 3.

3. Results and Discussion

3.1 Synthesis, Crystal Morphology, and Thermal Stability. As described in the experimental section, Mu-21 can be synthesized in the presence of ethylene glycol as solvent. This zincophosphate can also be prepared in an aqueous medium (sample A, Table 1). Such a result was unexpected because Mu-21 was previously obtained by dehydration of the zincophosphate Mu-19.[7] The latter material, prepared from a similar mixture (same organic template), displays a 3-D framework, and the removal of water by heating the sample at 80 °C leads to an unknown phase A which corresponds to Mu-21. It should be noted that the phase transformation is completely reversible. Under wet atmosphere (aqueous NH_4Cl saturated solution), Mu-21 adsorbs some water molecules (5 wt %) and is transformed into Mu-19. Therefore, after synthesis, Mu-21 has to be kept intact in a desiccator under P_2O_5 to preserve the structure and to avoid its rehydration. On Figure 2 are plotted the powder X-ray diffraction patterns of Mu-21 obtained by direct synthesis and recorded after dehydration of Mu-19 under P_2O_5 during 12 days at room temperature. For comparison, the XRD patterns of Mu-19 are also reported. These results prove that this drying condition is not sufficient to achieve a full dehydration, but under heating at 80 °C the dehydration is complete. The synthesis can be performed in the presence of F^- (sample C, Table 1) but in that case and contrary to what is observed for the synthesis of gallophosphates[11] F^- does not play a significant role.

The crystal size strongly depends on the solvent used during the synthesis. As expected, the crystals are smaller when the synthesis is performed in the presence of ethylene glycol (Figure 3b). When Mu-21 is synthesized in aqueous medium the crystal surfaces are rough, which may be explained by a partial crumbling of large crystals into smaller ones as it is clearly visible in Figure 3a and c.

(8) Werner, P. E.; Eriksson, L.; Westdhal, M. *J. Appl. Crystallog.* **1985**, *18*, 367−370.
(9) (a) Altomare, A.; Burla, M. C.; Cascarano, G.; Giacovazzo, C.; Guagliardi, A.; Moliterni, A. G. G.; Polidori, G. *J. Appl. Cryst.* **1995**, *28*, 842−846. (b) Altomare, A.; Cascarano, G.; Giacovazzo, C.; Guagliardi, A.; Burla, M. C.; Polidori, G.; Camalli, M. *J. Appl. Cryst.* **1994**, *27*, 435−436.
(10) Larson, A. C.; Von Dreele, R. B.; Lujan, M. *LANSCE, MS-H 805*; Los Alamos National Laboratory: Los Alamos, NM, 2000.
(11) Merrouche, A.; Patarin, J.; Kessler, H.; Soulard, M.; Delmotte, L.; Guth, J. L.; Joly, J. F. *Zeolites* **1992**, *12*, 226−232.

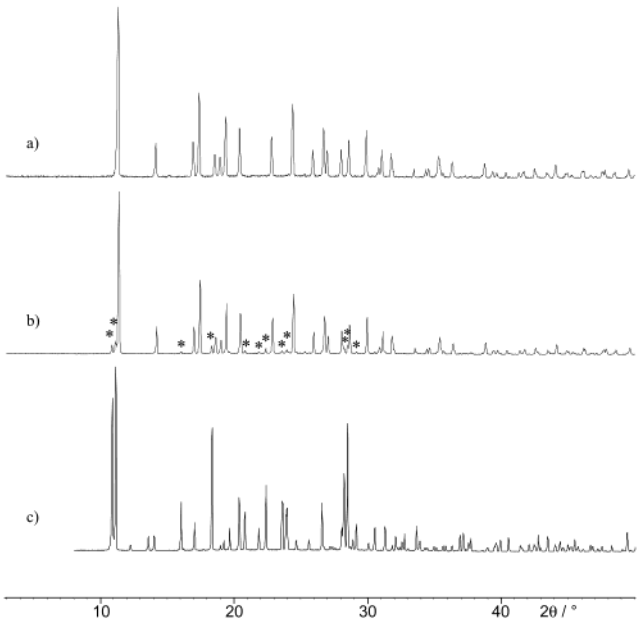

Figure 2. XRD patterns of (a) Mu-21, (b) Mu-21 after dehydration of Mu-19 under P_2O_5 during 12 days at room temperature (*: traces of Mu-19), and (c) Mu-19.

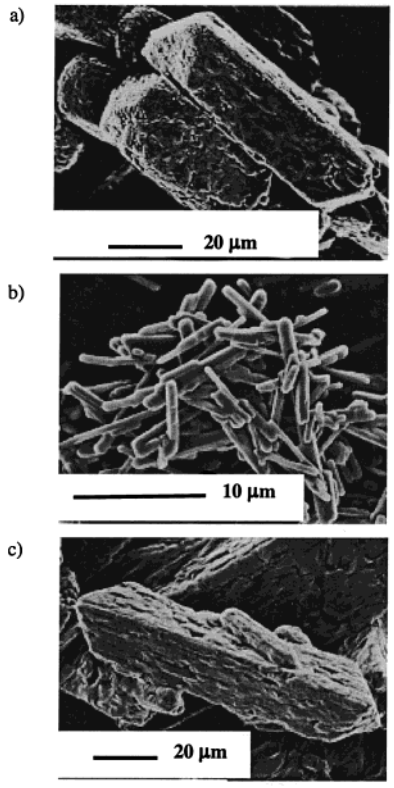

Figure 3. Scanning electron micrographs of some crystals of the zincophosphate Mu-21: (a) sample A, (b) sample B, and (c) sample C of Table 1.

As mentioned above, the synthesis conditions of Mu-19 and Mu-21 in aqueous medium are quite similar. The temperature conditions and the addition rate of the reactants may significantly change the result of the synthesis.

The analysis by high-temperature XRD performed under air shows that the structure of Mu-21 begins to collapse between 120 and 170 °C. The sample heated at 210 °C is amorphous.

3.2 Structure Determination. The powder X-ray pattern of Mu-21 was indexed in the orthorhombic symmetry with the following unit cell parameters: a = 10.42(1) Å, b = 10.45(1) Å, and c = 11.62(1) Å. The analysis of systematically extinguished reflections indicated the same space group as Mu-19, i.e. $P2_12_12_1$. The idealized unit cell chemical composition of Mu-21 is $(C_5H_{12}NO)_4Zn_4P_8O_{32}H_{12}$ and corresponds to a simple dehydration of Mu-19. In addition to the synthesis experimental results, this clearly suggested that the structure of Mu-21 must be closely related to that of Mu-19. For this reason the first attempts to solve the structure of Mu-21 were made by starting from Mu-19 after removal of the water molecules using energy minimization calculations performed with the Cerius[2] molecular modeling system.[12] Because of the large flexibility of the zincophosphate frameworks of Mu-19 and a fortiori Mu-21 which allowed a high number of possible energy minima, solving the structure with such a procedure was unsuccessful. Therefore, direct methods were applied to the integrated intensities as extracted from the powder X-ray data (see Experimental Section).

Successive calculated Fourier maps revealed the structure, i.e., framework atoms and the *N*-methylmorpholinium cation except the hydrogen atoms. An energy minimization performed with the Cerius2[12] software was used for the location of the hydrogen atoms by fixing all the non-hydrogen atoms. Then, the model was good enough to be introduced as a starting model for the Rietveld analysis. During the Rietveld refinement, restraints on the bond lengths and angles of the framework atoms were applied and an adequate set of soft constrains to transform the organic cation to a pseudo-rigid body was defined. At the end of the refinement, the reliability factors converged to the following values: R_p = 0.0370 and wR_p = 0.0459. The profile fit is given in Figure 4. Atomic coordinates, displacement parameters, and site occupation factors are given in Table 4. Selected bond lengths and angles are reported in Table 5.

3.3 Structure Description. As for Mu-19, the asymmetric unit of Mu-21 contains two nonequivalent phosphorus atoms, one zinc atom, and one *N*-methylmorpholinium cation. Both inorganic frameworks have the same distribution of the hydroxyl groups on the phosphorus atoms.

The average ⟨Zn−O⟩ and ⟨P−O⟩ distances are 1.918 and 1.520 Å, respectively. Except for the oxygen atoms O1, O2, O4, and O5 which are also bonded to zinc atoms, the shorter P−O distance, P3−O6 of 1.500(5) Å, corresponds to a phosphorus atom doubly bonded to an oxygen atom as previously observed for other zincophosphates.[7,13] The other distances P2−O3 = 1.502(8) Å, P2−O8 = 1.530(7) Å, and P3−O7 = 1.527(6) Å are representative of terminal hydroxyl groups as observed in Mu-19.

The phosphorus tetrahedra are quite regular with O−P−O angles in the range 106.1(5)−113.9(5)° with an average of 109.5°. These values are very similar to those

(12) Accelrys Inc. *Cerius[2] Modeling Environment, Release 4.2MS*. Accelrys Inc.: San Diego, CA, 2000.

(13) (a) Patarin, J.; Marler, B.; Huve, L. *Eur. J. Solid State Inorg. Chem*. **1994**, *31*, 909−920. (b) Ahmadi, K.; Hardy, A.; Patarin, J.; Huve, L. *Eur. J. Solid State Inorg. Chem*. **1995**, *32*, 209−223.

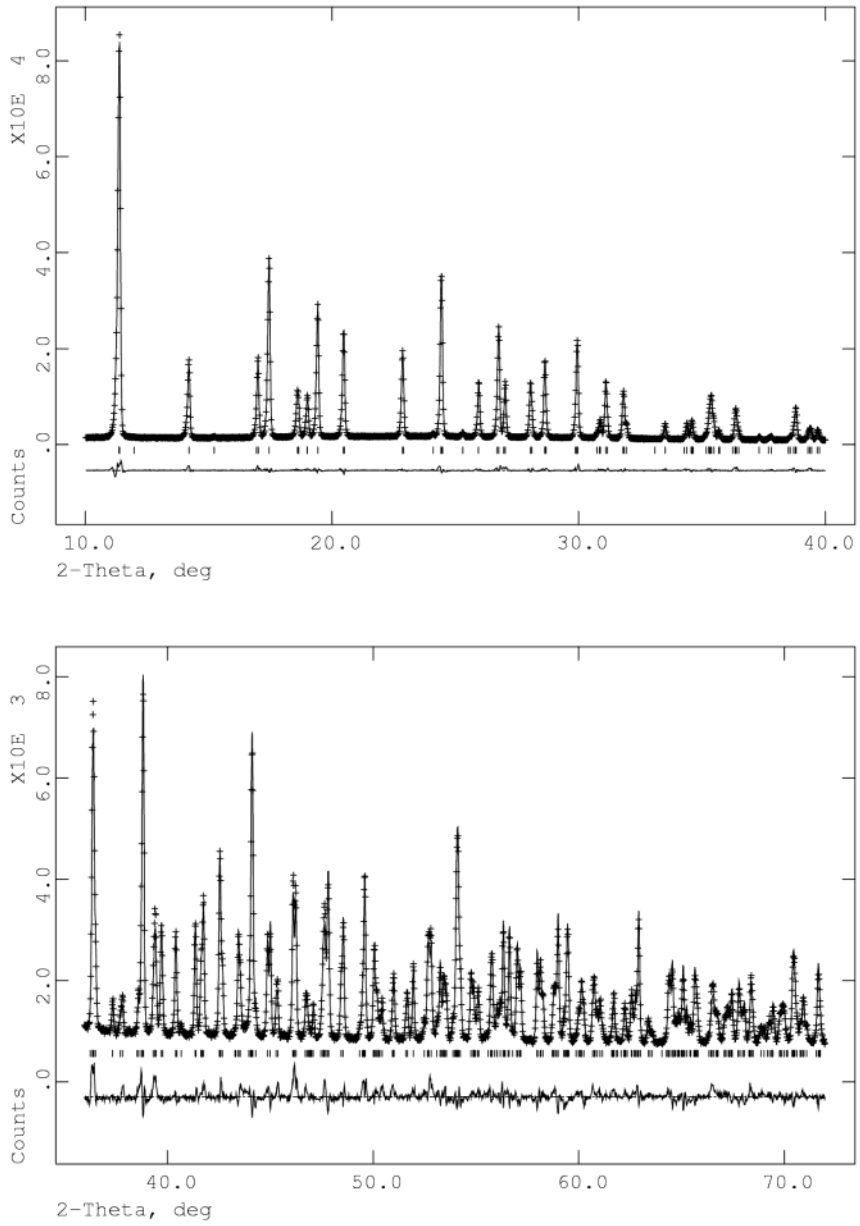

Figure 4. Rietveld refinement of Mu-21: experimental (crosses), calculated (full line), and difference plot (bottom line). The short vertical lines mark the positions of possible Bragg reflections.

observed in Mu-19 (average angle 109.4°, ranges from 105.3(3)−114.5(3)°). The ZnO_4 tetrahedra are also distorted with O−Zn−O angles in the range 99.9(5)−114.9(3)° [Mu-19: 99.9(2)−115.1(2)°].

The absence of the water molecules in Mu-21 has induced a new repartition of the hydrogen bonds inside the pores as described in Figure 5. An examination of the distances involved in both hydrogen bonding schemes shows that the organic molecules control the building of the zincophosphate framework and the shape of the twelve-membered rings through the phosphate hydroxyl groups. Indeed, in both structures, Mu-19 and Mu-21, the *N*-methylmorpholinium cations are located in the plane of the 12-membered rings but the organic molecule is more strongly bonded to the framework in the case of Mu-19 (Mu-19, O4···Hn = 1.886(1) Å; Mu-21, O1···Hn = 2.32(2) Å, O5···Hn = 2.45(2) Å). It is worthy to note that in Mu-19 the connection between the water molecules, the oxygen atom of the organic molecule, and the hydroxyl group are strong (O···H2 = 1.603(1) Å, O1w···H8 = 1.502(1) Å, O7···H1 = 1.800(1) Å) compared to the strength of the Hn···O4 bonds (1.886(1) Å) (Figure 5a). In the case of Mu-21, the organic molecules are strongly bonded to the framework via one hydroxyl hydrogen (O···H7 = 2.01(6) Å) while the hydrogen of the ammonium cation is connected to O1 and O5 oxygen atoms.

The three-dimensional interrupted framework of Mu-21 is similar to that of Mu-19. It consists of only twelve-membered rings which form a network of interconnected channels in all directions. These different types of channels are better viewed down the [1 0 0], [0 1 0], [1 1 1], [−1 1 1], [1 −1 1], and [1 1 −1] directions (Figure 6).

3.4 Solid State NMR Spectroscopy. The measurements of ^{31}P relaxation time (T_1) values show two different phosphorus populations present in approximately the same proportions (43% and 57%) and associated to T_1 values of 1.3 and 258 s, respectively. These populations are characterized by chemical shift

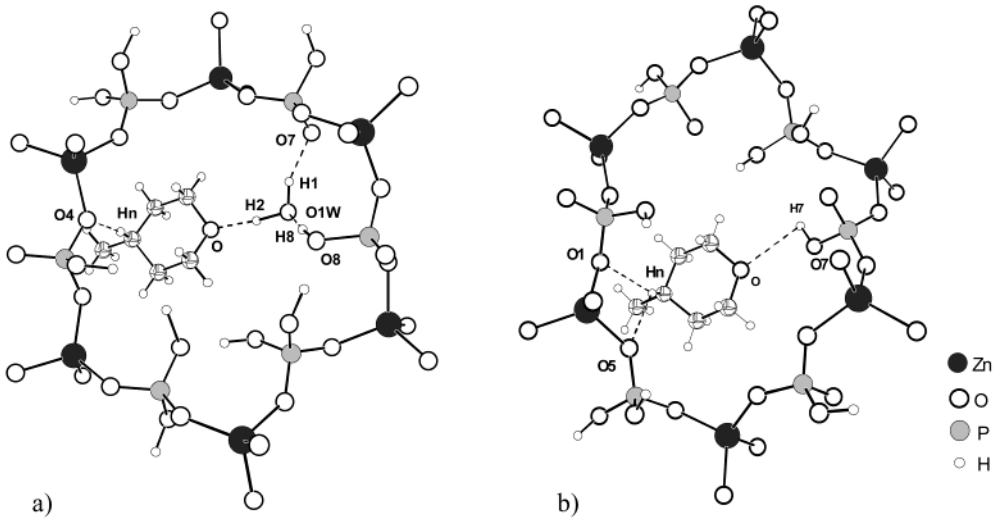

Figure 5. Hydrogen bonding schemes in (a) Mu-19 and (b) Mu-21.

Table 4. Atomic Parameters, Isotropic Displacement Parameters, U_i, and Occupation Factors for Mu-21 (Standard Deviations in Brackets)

atom	*x*	*y*	*z*	$U_i \times 100$	occup.
Zn1	.5531(2)	.2006(2)	.1188(2)	.68(3)[a]	1
P2	.3123(4)	.1601(5)	−0.0449(4)	.68(3)[a]	1
P3	.5132(4)	.4276(4)	.3006(4)	.68(3)[a]	1
O1	.4394(8)	.5489(8)	.2951(7)	1.9(1)[b]	1
O2	.4786(7)	.3371(8)	.2056(7)	1.9(1)[b]	1
O3	.2448(8)	.1146(10)	.0617(8)	1.9(1)[b]	1
O4	.4547(8)	.1897(8)	−0.0199(7)	1.9(1)[b]	1
O5	.2371(7)	.2734(8)	−0.0884(8)	1.9(1)[b]	1
O6	.6545(6)	.4552(9)	.3008(9)	1.9(1)[b]	1
O7	.4824(8)	.3653(8)	.4161(6)	1.9(1)[b]	1
O8	.3120(7)	.0536(8)	−0.1351(8)	1.9(1)[b]	1
C1	.447(1)	.554(1)	.964(1)	3.9(7)	1
C2	.464(1)	.481(1)	.853(1)	4.9(7)	1
C3	.343(1)	.643(1)	.755(1)	3.6(7)	1
C4	.328(1)	.709(1)	.870(1)	3.1(6)	1
C5	.369(1)	.432(1)	.667(1)	4.2(7)	1
N	.353(1)	.503(1)	.776(1)	2.2(5)	1
O	.436(1)	.686(1)	.940(1)	3.4(4)	1
Hn[d]	.281(1)	.476(2)	.812(1)	7(1)[c]	1
H1a[d]	.519(3)	.540(2)	1.013(2)	7(1)[c]	1
H1b[d]	.371(3)	.525(2)	1.002(2)	7(1)[c]	1
H2a[d]	.472(3)	.391(1)	.869(2)	7(1)[c]	1
H2b[d]	.541(1)	.511(3)	.815(2)	7(1)[c]	1
H3a[d]	.419(2)	.673(2)	.717(2)	7(1)[c]	1
H3b[d]	.5531(2)	.2006(2)	.1188(2)	.68(3)[a]	1
H4a[d]	.3123(4)	.1601(5)	−0.0449(4)	.68(3)[a]	1
H4b[d]	.5132(4)	.4276(4)	.3006(4)	.68(3)[a]	1
H5a[d]	.4394(8)	.5489(8)	.2951(7)	1.9(1)[b]	1
H5b[d]	.4786(7)	.3371(8)	.2056(7)	1.9(1)[b]	1
H5c[d]	.2448(8)	.1146(10)	.0617(8)	1.9(1)[b]	1
H3[d]	.4547(8)	.1897(8)	−0.0199(7)	1.9(1)[b]	1
H7[d]	.2371(7)	.2734(8)	−0.0884(8)	1.9(1)[b]	1
H8[d]	.6545(6)	.4552(9)	.3008(9)	1.9(1)[b]	1

[a,b,c] Parameters with the same superscript were constrained to be equal. [d] The hydrogen positions were placed with geometrical constraints.

values of 0.44 and 0.75 ppm, respectively (Figure 7). It is easier to distinguish the two crystallographic phosphorus populations in Mu-19 than in Mu-21. Indeed, in the former case, two peaks situated at 4.4 and −1.7 ppm were observed and assigned to ($PO_2(OH)_2$) and (PO_2O-(OH)), respectively. Therefore, the zincophosphate framework of the anhydrous structure (Mu-21) is seemingly slightly more relaxed then the framework of the hydrous precursor (Mu-19).

Table 5. Selected Bond Lengths and Angles for the Zincophosphate Mu-21

atoms	distances (Å)	atoms	angle (deg)
Zn1−O1	1.877(8)	O1−Zn1−O2	111.4(9)
Zn1−O2	1.912(8)	O1−Zn1−O4	114.9(3)
Zn1−O4	1.914(8)	O1−Zn1−O5	99.9(5)
Zn1−O5	1.968(7)	O2−Zn1−O4	105.8(3)
		O2−Zn1−O5	112.8(4)
		O4−Zn1−O5	112.3(4)
P2−O3	1.502(8)	O3−P2−O4	111.1(5)
P2−O4	1.543(7)	O3−P2−O5	106.4(5)
P2−O5	1.507(7)	O3−P2−O8	109.5(5)
P2−O8	1.530(7)	O4−P2−O5	113.9(5)
		O4−P2−O8	106.1(5)
		O5−P2−O8	109.9(5)
P3−O1	1.485(8)	O1−P3−O2	112.5(5)
P3−O2	1.497(7)	O1−P3−O6	110.2(5)
P3−O6	1.500(5)	O1−P3−O7	107.0(5)
P3−O7	1.527(6)	O2−P3−O6	111.1(5)
		O2−P3−O7	109.2(5)
		O6−P3−O7	106.7(6)
		Zn1−O1−P3	132.6(6)
		Zn1−O2−P3	139.7(5)
		P2−O3−H3	117(3)
		Zn1−O4−P2	133.5(5)
		Zn1−O5−P2	132.4(5)
		P3−O7−H7	119(5)
		P2−O8−H8	125(3)
O−C1	1.414(9)	C4−C3−N	108.1(7)
O−C4	1.408(9)	C1−C2−N	109.6(7)
C1−C2	1.508(9)	C2−N−C3	108.0(6)
C3−C4	1.508(9)	O−C1−C2	109.4(7)
N−C2	1.485(1)	O−C4−C3	110.5(8)
N−C3	1.485(1)	C1−O−C4	110.6(9)
N−C5	1.485(1)	C2−N−C5	109.9(7)
		C3−N−C5	111.1(7)
Hn-N	0.90(1)	H3···O6	1.72(4)
H1a−C1	0.96(1)	H7···O	2.01(6)
H1b−C1	0.96(1)	H8···O6	1.89(6)
H2a−C2	0.96(1)	Hn···O1	2.32(2)
H2b−C2	0.96(1)	Hn···O5	2.45(2)
H3a−C3	0.96(1)	H3−O3	1.01(2)
H3b−C3	0.96(1)	H7−O7	0.99(2)
H4a−C4	0.96(1)	H8−O8	0.98(2)
H4b−C4	0.96(1)		
H5a−C5	0.96(1)		
H5b−C5	0.96(1)		
H5c−C5	0.96(1)		

Figure 8a shows the ^{1}H MAS NMR spectrum of Mu-21. To assign the different peaks, Mu-21 was placed in a D_2O atmosphere during 7 h at room temperature in order to induce a proton−deuterium exchange.

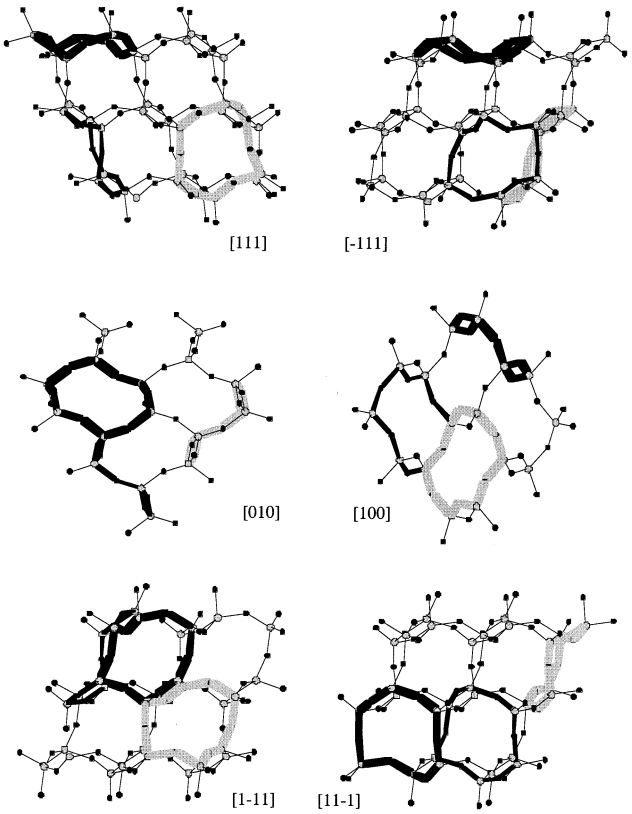

Figure 6. Views of Mu-21 down the six directions showing the different straight interconnected 12-membered rings channels. Three types of 12-membered rings are represented in thick lines (two in black with different thickness and one in gray) in each different direction.

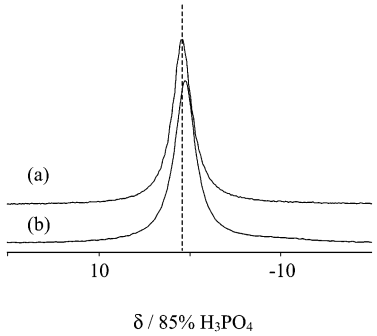

Figure 7. ^{31}P MAS NMR spectra of the zincophosphate Mu-21 recording with a recycle time of (a) 6 s and (b) 1032 s.

Adsorbed D_2O molecules were evacuated at 80 °C for one night and the new sample was named D-Mu-21. The ^{1}H MAS NMR spectrum of this last sample is reported in Figure 8b and it is representative of protons that were not exchanged. On the other hand, the peaks associated to the proton populations that were exchanged with deuterium are shown in Figure 8c. Three peaks can be observed at 8.9, 3.6, and 2.3 ppm in the proportions 27.3, 23.2, and 49.5%, respectively. They can be attributed to protons of the ammonium cation, the $PO_2O(OH)$ group, and the $PO_2(OH)_2$ group, respectively, in agreement with the structure determination. The thickness of the peak situated at 2.3 ppm ($\Delta\nu_{1/2}$ = 0.53 ppm) confirms that protons of the $PO_2(OH)_2$ groups are not involved in the hydrogen bonding scheme contrary to the proton of the $PO_2O(OH)$ group (3.6 ppm, $\Delta\nu_{1/2}$ = 2.61 ppm). The identification of the other peaks (Figure 8b) is more difficult because the exchange might not be complete: they correspond to protons of the CH_2 and CH_3 groups of the ammonium cation but also to protons that are involved in the hydrogen bonding scheme.

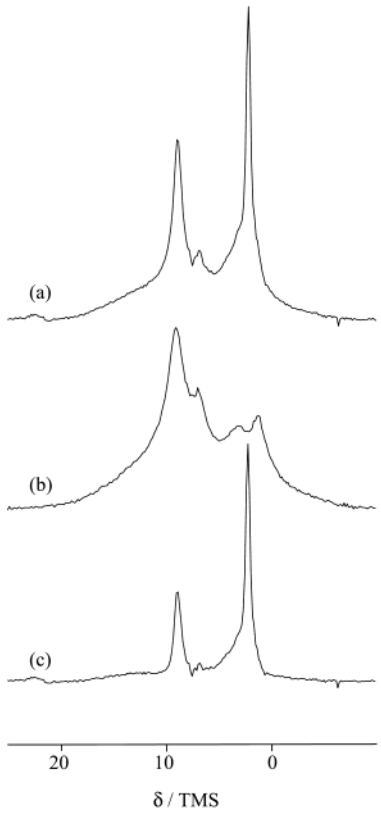

Figure 8. ^{1}H MAS NMR spectra of (a) the zincophosphate Mu-21, (b) D-Mu-21, and (c) spectrum difference [(a − b)].

4. Conclusion

The zincophosphate Mu-21 can be synthesized in the presence of different solvents (water or ethylene glycol) and with *N*-methylmorpholine as organic structure-directing agent. Although it was obtained in aqueous medium, no water molecule was located inside the channels. The hydration of the sample does not induce a collapsing of the structure as it is rather the case for zincophosphates but it allows to obtain (reversibly) the zincophosphate Mu-19. In the zincophosphate system, Mu-21 and Mu-19 prove how important the synthesis procedure is.

Acknowledgment. We thank Ludovic Josien for fruitful discussions.

CM021330G